

Conformal Gravity Rotation Curves with a Conformal Higgs Halo

Keith Horne¹

¹*SUPA Physics and Astronomy, University of St. Andrews, KY16 9SS, Scotland, UK*

Accepted . Received ; in original form

ABSTRACT

We discuss the effect of a conformally coupled Higgs field on conformal gravity (CG) predictions for the rotation curves of galaxies. The Mannheim-Kazanas (MK) metric is a valid vacuum solution of CG's 4-th order Poisson equation only if the Higgs field has a particular radial profile, $S(r) = S_0 a/(r + a)$, decreasing from S_0 at $r = 0$ with radial scale length a . Since particle rest masses scale with $S(r)/S_0$, their world lines do not follow time-like geodesics of the MK metric $g_{\mu\nu}$, as previously assumed, but rather those of the Higgs-frame MK metric $\tilde{g}_{\mu\nu} = \Omega^2 g_{\mu\nu}$, with the conformal factor $\Omega(r) = S(r)/S_0$. We show that the required stretching of the MK metric exactly cancels the linear potential that has been invoked to fit galaxy rotation curves without dark matter. We also formulate, for spherical structures with a Higgs halo $S(r)$, the CG equations that must be solved for viable astrophysical tests of CG using galaxy and cluster dynamics and lensing,

Key words: (gravitation, galaxies: kinematics and dynamics, cosmology: theory, dark matter, dark energy)

1 INTRODUCTION

The need for dark matter and dark energy to reconcile Einstein's General Relativity (GR) with observations, together with the lack of other tangible evidence for their existence, motivates the study of alternative gravity theories aiming to achieve similar success without resort to the dark sector.

Conformal Gravity (CG), like GR, employs a metric to describe gravity as curved space-time. But the CG field equations, which dictate how matter and energy generate space-time curvature, arise from a local symmetry principle, conformal symmetry, which holds for the strong, weak and electro-magnetic interactions, but is violated by GR. Conformal symmetry means that stretching the metric by a factor $\Omega^2(x)$, and scaling all other fields by appropriate powers of Ω , has no physical effects. In particular, local conformal transformations preserve all angles and the causal relations among space-time events, but physical distances, time intervals, and masses change, so that only local ratios of these quantities have physical significance.

Unlike GR, and many related alternative gravity theories, terms allowed in the CG action are highly restricted by the required conformal symmetry. GR's Einstein-Hilbert action adopts the Ricci scalar \mathcal{R} , leading to Einstein's famous 2nd-order field equations,

$$G_{\mu\nu} + \Lambda g_{\mu\nu} = -8\pi G T_{\mu\nu} , \quad (1)$$

where $G_{\mu\nu} = R_{\mu\nu} - (\mathcal{R}/2) g_{\mu\nu}$ is the Einstein tensor, G is Newton's constant, and Λ is the cosmological constant. These terms are excluded in CG because Λ and G build in fundamental scales, and \mathcal{R} violates conformal symmetry. Instead the CG action allows only conformally-invariant scalars linked by dimensionless coupling constants. \mathcal{R} can appear if it is coupled to a scalar field S in the particular conformally-invariant combination $S^{;\mu} S_{;\mu} - \frac{\mathcal{R}}{6} S^2$. Particle rest masses cannot be fundamental, but may instead arise through Yukawa couplings to the conformal Higgs field S . Likewise, the Higgs mass cannot be fundamental, but may arise through dynamical symmetry breaking. Conformal invariance replaces Einstein's 2nd-order field equations with the 4th-order CG field equations (Mannheim & Kazanas 1989; Mannheim 2006),

$$4\alpha W_{\mu\nu} = T_{\mu\nu} , \quad (2)$$

where α is a dimensionless coupling constant. The Bach tensor $W_{\mu\nu}$ and stress-energy tensor $T_{\mu\nu}$ are both traceless, and scale as Ω^{-4} .

Despite their complexity, the 4th-order CG field equations admit analytic solutions for systems with sufficient symmetry (Mannheim 2006). For homogeneous and isotropic space-times (Mannheim 2001), the Robertson-Walker metric is a solution with $W_{\mu\nu} = 0$, providing a dynamical cosmological model identical to that of GR, except

that the Friedmann equation has a negative effective gravitational constant $G_{\text{eff}} = -3/4 \pi S_0^2$, where S_0 is the vacuum expectation value of a conformally-coupled scalar field with vacuum energy density λS_0^4 . This CG cosmology gives an open universe, but it can fit luminosity distances from supernovae (Mannheim 2003) and features cosmic acceleration with $0 < \Omega_\Lambda < 1$, neatly solving the cosmological constant problem without dark energy (Mannheim 2001; Mannheim 2011), see also (Nesbet 2011). Growth of structure in CG cosmology is starting to be investigated (Mannheim 2012), but has not yet produced predictions for the CMB.

The plan of this paper is as follows: In Sec. 2 we review the static spherical solutions that have been used with some success (Mannheim 1993; Mannheim 1997; Mannheim & O'Brien 2012) to fit the rotation curves of spiral galaxies, large and small. In Sec. 3 we discuss the need for a conformally coupled Higgs field $S(r)$, and show that it makes a non-zero contribution to the source $f(r)$ in CG's 4th-order Poisson equation unless it has a particular radial profile $S(r) = S_0 a/(r+a)$. In Sec. 4 we stretch the MK metric with the conformal factor $\Omega_S(r) = S(r)/S_0$, and show that the linear potential used in previous fits to galaxy rotation curves is effectively removed. In Sec. 5 we summarise the coupled system of equations that must be solved in order to make astrophysical tests of CG predictions for static spherically symmetric structures. We summarise and conclude in Sec. 6.

2 STATIC SPHERICAL SOLUTIONS

For static and spherically symmetric spacetime geometries, analytic solutions to CG include the Mannheim-Kazanas metric (Mannheim & Kazanas 1989) (MK), an extension of GR's Schwarzschild metric.

Co-moving coordinates render W_ν^μ and T_ν^μ diagonal, giving in principle 4 CG field equations. But only 2 are independent, given that spherical symmetry requires $W_\theta^\theta = W_\phi^\phi$, and the Bianchi identities require a traceless Bach tensor, $W_\mu^\mu = 0$, and hence $T_\mu^\mu = 0$.

MK show that for any static spherically symmetric spacetime, a particular conformal transformation brings the metric into a standard form ^{*},

$$ds^2 = -B(r) dt^2 + \frac{dr^2}{B(r)} + r^2 d\theta^2 + r^2 \sin^2 \theta d\phi^2. \quad (3)$$

We refer to this standard form, in which $-g_{00} = g_{rr} = B(r)$, as the "MK frame".

With this metric ansatz, MK show that the CG field equations boil down to an exact 4th-order Poisson equation for $B(r)$:

$$\frac{3}{B} (W_0^0 - W_r^r) = \frac{1}{r} (r B)'''' = \frac{3}{4\alpha B} (T_0^0 - T_r^r) \equiv f(r), \quad (4)$$

where $'$ denotes d/dr , and $f(r)$ is the CG source. Note that $T_0^0 = -\rho$ and $T_r^r = p$ for a perfect fluid (representing matter and radiation) with energy density ρ and pressure p .

The remaining constraint can then be the 3rd-order equation

$$W_r^r = \frac{1-B^2}{3r^4} + \frac{2BB'}{3r^3} - \frac{BB'' + (B')^2}{3r^2} + \frac{B'B'' - BB'''}{3r} + \frac{2B'B''' - (B'')^2}{12} = \frac{1}{4\alpha} T_r^r, \quad (5)$$

which can be imposed as a boundary condition (Brihaye & Verbin 2009).

2.1 Vacuum Solution : The MK metric

A *source-free* vacuum solution requires $T_0^0 = T_r^r$, so that $f(r)=0$. Since

$$(r^{n+1})'''' = (n+1)n(n-1)(n-2)r^{n-3} \quad (6)$$

vanishes for $n = -1, 0, 1$, and 2 , the homogeneous 4th-order Poisson equation then integrates 4 times to give

$$B(r) = w - \frac{2\beta}{r} + \gamma r - \kappa r^2, \quad (7)$$

with 4 integration constants w, β, γ and κ . The 3rd-order constraint $4\alpha W_r^r = T_r^r$ then gives

$$w^2 = 1 - 6\beta\gamma + \frac{3r^4}{4\alpha} T_r^r. \quad (8)$$

For $T_r^r = 0$, or $T_r^r \propto r^{-4}$, this gives 1 constraint on the 4 coefficients, leaving the metric with 3 parameters: β, γ, κ .

This Mannheim-Kazanas (MK) metric matches the successes of GR's Schwarzschild metric in the classic solar system tests, if we identify $\beta = M$ and require $|\beta\gamma| \ll 1$. The quadratic potential, $-\kappa r^2$, embeds the spherical structure into a curved space at large r .

2.2 Rotation Curves

The MK metric's linear potential, γr , enjoys some success in fitting galaxy rotation curves (Mannheim & O'Brien 2012). For circular orbits, the rotation curve for the MK metric is

$$v^2 \equiv \frac{r^2 \dot{\theta}^2}{B} = \frac{d \ln(|g_{00}|)}{d \ln(|g_{\theta\theta}|)} = \frac{r B'}{2B} = \frac{\frac{\beta}{r} + \frac{\gamma}{2} r - \kappa r^2}{w - \frac{2\beta}{r} + \gamma r - \kappa r^2}. \quad (9)$$

Fig. 1 shows the metric potential $B(r)$ and the corresponding rotation curve $v(r)$ for a compact point mass $M = \beta = 10^{11} M_\odot$. In the weak field limit relevant to astrophysics, $B \approx 1$, so that the three terms in the numerator of Eqn. (9) determine the shape of the velocity curve. The Newtonian potential $-2\beta/r$ gives a Keplerian rotation curve $v^2 = \beta/r$. The linear potential γr gives a rising rotation curve $v^2 = \gamma r/2$. A flat rotation curve resembling those observed on the outskirts of large spiral galaxies (Rubin, Ford, Thonnard 1978) then corresponds to the transition between these regimes, at $r^2 \sim 2\beta/\gamma$, or $r \sim 19$ kpc for the case in Fig. 1. The velocity at the transition radius, $v \approx (2\beta\gamma)^{1/4}$, can approximate the observed Tully-Fisher relation $v^4 \propto M$ (Tully & Fisher 1977), provided γ has the right magnitude and is independent of β .

To fit the rising rotation curves observed in smaller dwarf galaxies, however, it is necessary to assume a relationship between γ and M :

$$\gamma(M) = \gamma_0 + \gamma_\star \left(\frac{M}{M_\odot} \right) = \gamma_0 \left(1 + \frac{M}{M_0} \right), \quad (10)$$

^{*} Here and henceforth we adopt natural units with $\hbar = c = G = 1$.

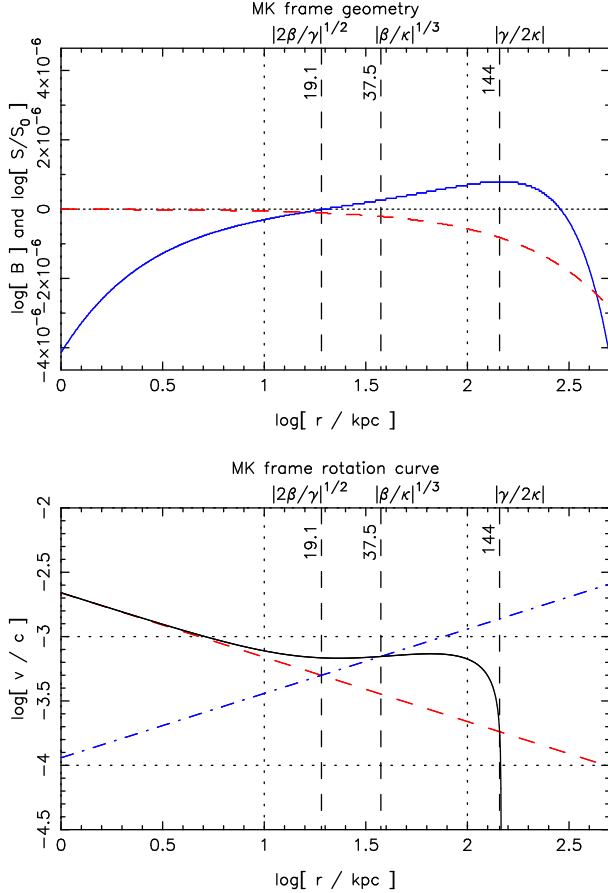


Figure 1. Top panel: The MK metric potential $B(r) = w - 2\beta/r + \gamma r - \kappa r^2$ (blue curve) and the associated Higgs halo $S(r)$ (red dashed) for a point mass $\beta = M = 10^{11} M_\odot$, with the MK parameters (β, γ, κ) used by (Mannheim & O’Brien 2012) to fit the rotation curves of spiral galaxies. Bottom panel: Circular orbit velocity curve $v^2 = rB'/2B$ for the MK potential $B(r)$ (black curve), $v^2 = \beta r/B$ for the Newtonian potential (red dashed) and $v^2 = \gamma r/2B$ for the linear potential (blue dot-dash). Three fiducial radii at transitions between the Newtonian, linear, and quadratic potentials are also marked. The rotation curve is relatively flat from 10 to 100 kpc as a result of cancelling contributions from the three potentials. The potential $B(r)$ has a maximum at the watershed radius $r = |\gamma/2\kappa| \approx 144$ kpc, outside which there are no stable circular orbits.

where M is the galaxy mass, $\gamma_0 = 3.06 \times 10^{-30} \text{ cm}^{-1}$, $\gamma_\star = 5.42 \times 10^{-41} \text{ cm}^{-1}$, and $M_0 \equiv \gamma_0/\gamma_\star = 5.6 \times 10^{10} M_\odot$. This metric fits the rotation curves of a wide variety of spiral galaxies, replacing their individual dark matter halos by just 2 free parameters (Mannheim 1993; Mannheim 1997).

To justify this particular form, it is argued (Mannheim 1993) that γ_0 is generated by matter external to r while γ_\star is generated by matter internal to r . This argument is plausible but in our view not really convincing until it becomes clearer how to calculate γ_0 given the external matter distribution in the expanding universe.

The most recent fits (Mannheim & O’Brien 2012) to a sample of 111 galaxies require invoking the quadratic potential $-\kappa r^2$ to counter the rising γr potential on the outskirts of particularly large galaxies like Malin 1. The required scale, $-\kappa = 9.54 \times 10^{-54} \text{ cm}^{-2} \sim -(100 \text{ Mpc})^{-2}$, is plausi-

bly identified with the observed size of typical structures in the cosmic web. For the $10^{11} M_\odot$ point mass illustrated in Fig. 1, the transition from rising linear to falling quadratic potential has the effect of extending the relatively flat part of the rotation curve out to around 100 kpc, and eliminating bound circular orbits outside the “watershed radius” $r = |\gamma/2\kappa|^{1/2} = 144$ kpc, where the potential $B(r)$ reaches a maximum.

2.3 Concerns about using the MK metric

Given the notable success of the MK metric in fitting a wide variety galaxy rotation curves with just 3 parameters, it is tempting to conclude that CG provides a simpler description of galaxy dynamics than an alternative model with hundreds of individual dark matter halos.

However, the vacuum has a non-zero Higgs field, with radial profile $S(r)$. This raises two potential problems with using the MK metric’s linear potential γr to fit galaxy rotation curves. First, with a non-constant $S(r)$, test particles find their rest masses changing with position, causing them to deviate from geodesics of the MK metric (Mannheim 1993b; Wood & Moreau 2001). Second, if $S(r)$ fails to satisfy $(1/S)'' = 0$, then $f(r)$ is non-zero, causing the MK coefficients w, β, γ, κ to be functions of r , and altering their radial dependence within and outside extended mass distributions such as galaxies and galaxy clusters.

The role of $S(r)$ in sourcing $B(r)$ has been previously investigated (Mannheim 2007; Brihaye & Verbin 2009), but the best CG analysis of galactic rotation curves to date (Mannheim & O’Brien 2012) omits this effect, arguing that it is negligible. In our view conclusions about the success of CG in fitting galaxy rotation curves are unsafe unless it can be justified to neglect radial gradients in $S(r)$. We argue below that even though $S(r)$ is very nearly constant, its radial gradient is large enough to significantly alter predictions for galaxy rotation curves, and moreover the effect on the rotation curve is to cancel that of the linear potential.

Null geodesics (photon trajectories) are independent of conformal transformations, and those of the MK metric are well studied (Edery & Paranjape 1998; Pireaux 2004; Sultana & Kazanas 2012; Villanueva & Olivares 2013). A major challenge to CG is that a linear potential with $\gamma r > 0$ is needed to fit galaxy rotation curves, and this produces light bending in the wrong direction, away from the central mass rather than toward it, making it difficult to account for observed gravitational lensing effects. However, since $S(r)$ affects $B(r)$, analysis of lensing by extended sources like galaxies and clusters must also include the Higgs halo. We show below that the Higgs halo $S(r)$ outside a point mass effectively eliminates the γr potential, so that rotation curves may no longer constrain the sign of γ . We may then reconsider using $\gamma < 0$ when analysing gravitational lensing effects.

3 CONFORMALLY COUPLED HIGGS FIELD

Vacuum solutions of GR, such as the Schwarzschild and Kerr metrics, assume $T^\mu_\nu = 0$, and the MK metric of CG assumes $f \propto T^0_0 - T^r_r = 0$. However, the vacuum now has a Higgs

field S , for which T_ν^μ and/or f may well not vanish. A family of analytic solutions of GR with a conformally-coupled scalar field (Wehus & Ravndal 2007) includes the extreme Reissner-Nordström black hole metric, with

$$B(r) = \left(1 - \frac{M}{r}\right)^2, \quad (11)$$

sourced by the scalar field profile

$$S(r) = \left(\frac{3}{4\pi}\right)^{1/2} \frac{M}{r-M}. \quad (12)$$

Below we discuss a similar solution for CG.

For the CG matter action

$$I_M = \int d^4x \sqrt{-g} \mathcal{L}_M, \quad (13)$$

the Lagrangian density (Mannheim 2007) is

$$\mathcal{L}_M = -\frac{1}{2} \left(S^{;\mu} S_{;\mu} - \frac{\mathcal{R}}{6} S^2 \right) - \lambda S^4 - \bar{\psi} (\mathcal{D} - h S) \psi. \quad (14)$$

This features a Dirac 4-spinor field ψ , with Dirac operator \mathcal{D} and Yukawa coupling to the conformal Higgs field S with dimensionless coupling constant h . Note that a conformal factor Ω stretches the volume element $\sqrt{-g} d^4x$ by Ω^4 , so that conformal symmetry requires $\mathcal{L}_M \propto \Omega^{-4}$. With $S \propto \Omega^{-1}$, conformal symmetry holds for the sum of the first two terms, for the quartic self-coupling potential λS^4 , and as well for the fermion terms with $\psi \propto \Omega^{-3/2}$.

Varying I_M with respect to ψ gives the Dirac equation

$$\mathcal{D} \psi = h S \psi, \quad (15)$$

with the fermion mass $m = h S$ induced by Yukawa coupling. Varying I_M with respect to S gives the 2nd-order Higgs equation of motion

$$S^{;\mu}_{;\mu} = \frac{1}{\sqrt{-g}} \left(\sqrt{-g} g^{\mu\alpha} S_{;\alpha} \right)_{;\mu} = -\frac{\mathcal{R}}{6} S + 4\lambda S^3 - h \bar{\psi} \psi. \quad (16)$$

This is the Klein-Gordon equation in curved spacetime, for a massless scalar field S with a fermion source $h \bar{\psi} \psi$ and a space-time dependent “Mexican hat” potential

$$V(S) = -\frac{\mathcal{R}}{12} S^2 + \lambda S^4. \quad (17)$$

Varying I_M with respect to the metric gives the conformal stress-energy tensor, with mixed components

$$T_\nu^\mu = T_\nu^\mu(\psi) + \frac{2}{3} S^{;\mu} S_{;\nu} - \frac{1}{3} S S^{;\mu}_{;\nu} - \frac{1}{6} S^2 \mathcal{R}_\nu^\mu - \delta_\nu^\mu \left(\frac{1}{6} S^{;\alpha} S_{;\alpha} - \frac{1}{3} S S^{;\alpha}_{;\alpha} - \frac{1}{12} \mathcal{R} S^2 + \lambda S^4 \right). \quad (18)$$

The trace

$$T_\alpha^\alpha = \bar{\psi} \mathcal{D} \psi + S S^{;\alpha}_{;\alpha} + \frac{1}{6} \mathcal{R} S^2 - 4\lambda S^4 \quad (19)$$

vanishes by virtue of the Higgs and Dirac equations.

For static spherically-symmetric fermion fields, the stress-energy tensor takes the form

$$T_\nu^\mu(\psi) = \text{diag}(-\rho, p_r, p_\perp, p_\perp), \quad (20)$$

with energy density ρ , radial pressure p_r , and azimuthal pressure p_\perp . The Dirac equation (15) then gives

$$h S \bar{\psi} \psi = \bar{\psi} \mathcal{D} \psi = p_r + 2p_\perp - \rho. \quad (21)$$

We can consider a Higgs field $S(r, t)$, allowing for a possible time dependence, with the understanding that the consequent stress-energy tensor and gravitational source $f(r)$ must be time independent for the static spherical structures of primary interest here. An example is a complex Higgs field with $S \propto e^{-i\omega t}$, for which $(\dot{S})^2 = -\omega^2 S^2$ and $\dot{S} = -\omega^2 S$.

Specialising to the MK metric, the Higgs equation (16) evaluates as

$$\frac{\ddot{S}}{B} = \frac{1}{r^2} (r^2 B S')' + \frac{\mathcal{R}}{6} S - 4\lambda S^3 + \frac{p_r + 2p_\perp - \rho}{S}, \quad (22)$$

with the Ricci scalar

$$\mathcal{R} = \frac{(r^2 B)'' - 2}{r^2} = \frac{2(w-1)}{r^2} + \frac{6\gamma}{r} - 12\kappa. \quad (23)$$

4 THE HIGGS FRAME

A conformal transformation Ω maps the Higgs field S to

$$S \rightarrow \tilde{S} = \Omega^{-1} S. \quad (24)$$

Transforming to the “Higgs frame”, where $\tilde{S} = S_0$, requires the specific conformal factor $\Omega_S(x) = S(x)/S_0$. In the static spherical geometry, given any CG solution $B(r)$ and $S(r)$ in the MK frame, where $-g_{00} = 1/g_{rr} = B(r)$, we can “stretch” the metric into the Higgs frame:

$$g_{\mu\nu} \rightarrow \tilde{g}_{\mu\nu} = \Omega^2 g_{\mu\nu} = \left(\frac{S}{S_0}\right)^2 g_{\mu\nu}. \quad (25)$$

In the Higgs frame, test particles have space-time independent rest masses, $\tilde{m} = h S_0$, and thus they follow geodesics of this stretched metric $\tilde{g}_{\mu\nu}$, rather than those of the MK metric $g_{\mu\nu}$.

4.1 Vacuum Stability and Spontaneous Symmetry Breaking

Using a tilde to denote the Higgs-frame counterparts of the MK-frame Higgs and fermion fields, we have $\tilde{S} = \Omega^{-1} S = S_0$, and $\tilde{\psi} = \Omega^{-3/2} \psi = (S/S_0)^{-3/2} \psi$. The fermion stress-energy components are then $(\tilde{\rho}, \tilde{p}_r, \tilde{p}_\perp) = (\rho, p_r, p_\perp) (S/S_0)^{-4}$. The MK-frame Higgs equation is then

$$\frac{\ddot{\tilde{S}}}{B} = \frac{1}{r^2} (r^2 B \tilde{S}')' + \frac{\mathcal{R}}{6} \tilde{S} - \left(4\lambda + \frac{\tilde{\rho} - \tilde{p}_r - 2\tilde{p}_\perp}{S_0^4} \right) \tilde{S}^3. \quad (26)$$

The fermions effectively increase the quartic Higgs self-coupling constant from λ to

$$\tilde{\lambda} \equiv \lambda + \frac{\tilde{\rho} - \tilde{p}_r - 2\tilde{p}_\perp}{4 S_0^4}. \quad (27)$$

The corresponding Higgs potential is

$$V(S) = -\frac{\mathcal{R}}{12} S^2 + \tilde{\lambda} S^4 = \tilde{\lambda} \left(S^2 - \frac{\mathcal{R}}{24\tilde{\lambda}} \right)^2 - \frac{\mathcal{R}^2}{576\tilde{\lambda}}. \quad (28)$$

A stable vacuum requires $\tilde{\lambda} > 0$. Spontaneous symmetry breaking, inducing non-zero fermion masses, can then occur for positive curvature $\mathcal{R} > 0$. The minimum of $V(S)$ occurs at $S^2 = \mathcal{R}/24\tilde{\lambda}$. This gives the vacuum a negative energy density $V(S) = -\mathcal{R}^2/576\tilde{\lambda} = -\tilde{\lambda} S^4$.

4.2 Source-Free Solution : The BV Metric

The source $f(r)$ in CG's 4-th order Poisson equation includes both fermion and Higgs contributions (Mannheim 2007; Brihaye & Verbin 2009):

$$4\alpha f(r) = \frac{3}{B} (p_r - \rho) + S^3 \left(\left(\frac{1}{S} \right)'' + \frac{1}{B^2} \left(\frac{1}{S} \right)'' \right). \quad (29)$$

The Higgs field $S(r, t)$ makes no explicit contribution to $f(r)$ if and only if it takes the specific form

$$S(r, t) = \frac{S_0 t_0 a}{(t + t_0)(r + a)}, \quad (30)$$

declining from S_0 at time $t = 0$ and radius $r = 0$ with a timescale t_0 and radial length scale a .

The time dependence included here may have applications, for example when embedding static spherical structures in an expanding universe, with $t_0 \sim 1/H_0$, or for a complex Higgs field varying as $S(r, t) = S(r) e^{-i\omega t}$. We set $t_0 = \infty$ to focus on static solutions.

Note in Eqn. (29) that a static ‘‘Higgs halo’’ $S(r)$ makes a contribution to $f(r)$ that does not depend on $B(r)$. Thus when $S(r)$ is known it is straightforward to integrate the 4th-order Poisson equation (4) to determine the corresponding $B(r)$. One cannot specify an arbitrary $S(r)$, however, since $B(r)$ appears in the equation of motion (22) for $S(r)$. Remarkably, the MK potential $B(r)$ and source-free $S(r)$ do admit an analytic solution (Brihaye & Verbin 2009), as we see below.

(Brihaye & Verbin 2009) (BV) use numerical methods to investigate static spherical solutions of CG with various assumptions about $f(r)$. Among these BV identify one 3-parameter analytic solution with a source-free scalar field,

$$S(r) = \frac{S_0 a}{r + a}, \quad (31)$$

for which the MK potential is

$$B(r) = \left(\frac{a+r}{a} \right)^2 \left(1 - \frac{\tilde{h}}{\tilde{r}(r)} \right) - K r^2 \left(1 - \frac{\tilde{h}^3}{\tilde{r}^3(r)} \right), \quad (32)$$

where $\tilde{h} \equiv h a / (a+h)$, $\tilde{r} \equiv r a / (a+r)$, and $K \equiv -2\lambda S_0^2$. This metric has a Schwarzschild-like horizon, with $B(r) \propto (r-h)$ vanishing at $r = h$.

Expanding Eqn. (32) in powers of r , we can read off the 3 independent MK parameters (β, γ, κ) in terms of the 3 BV parameters (h, a, K) :

$$2\beta = \tilde{h} (1 - K \tilde{h}^2), \quad (33)$$

$$\gamma = \frac{1}{a} \left(2 - 3 \frac{\tilde{h}}{a} (1 - K \tilde{h}^2) \right), \quad (34)$$

$$\kappa = K - \frac{1}{a^2} \left(1 - \frac{\tilde{h}}{a} (1 - K \tilde{h}^2) \right). \quad (35)$$

From these one can verify that the constant term,

$$w = 1 - 3 \frac{\tilde{h}}{a} (1 - K \tilde{h}^2) = \gamma a - 1 = 1 - \frac{6\beta}{a}, \quad (36)$$

satisfies the $W_r^r = 0$ constraint $w^2 = 1 - 6\beta\gamma$. The inverse relations are:

$$a = \frac{1+w}{\gamma} = \frac{6\beta}{1-w}, \quad (37)$$

$$K = \kappa + \left(\frac{\gamma}{1+w} \right)^2 - 2\beta \left(\frac{\gamma}{1+w} \right)^3, \quad (38)$$

and finally, the horizon radius h , where $B(r)$ vanishes, is the smallest positive real root of the cubic

$$0 = -2\beta + w r + \gamma r^2 - \kappa r^3. \quad (39)$$

The MK and BV metrics are thus equivalent, representing the same 3-parameter source-free solution to the CG field equations. However, as BV show, the Higgs field has a radial profile $S(r)$. Massive test particles therefore do not follow the time-like geodesics of the MK metric.

Fortunately, since we know $S(r)$, we know the conformal transformation between the MK frame and the Higgs frame:

$$S = \frac{S_0 a}{r + a} \rightarrow \tilde{S} = \Omega^{-1} S = S_0, \quad (40)$$

$$g_{\mu\nu} \rightarrow \tilde{g}_{\mu\nu} = \Omega^2 g_{\mu\nu} = \left(\frac{S}{S_0} \right)^2 g_{\mu\nu} = \left(\frac{a}{r+a} \right)^2 g_{\mu\nu}. \quad (41)$$

The stretched metric's circumferential radius

$$\tilde{r} \equiv \sqrt{|\tilde{g}_{\theta\theta}|} = \frac{r S}{S_0} = \frac{r a}{r + a} \quad (42)$$

maps $0 < r < \infty$ to $0 < \tilde{r} < a$. The stretched metric has

$$|\tilde{g}_{00}| = \left(\frac{a}{r+a} \right)^2 B(r) = 1 - \frac{2M}{\tilde{r}} - K \tilde{r}^2, \quad (43)$$

featuring a Newtonian potential with mass

$$M = \frac{h}{2} (1 + K h^2) \quad (44)$$

embedded in an external space with curvature K . The conformal transformation does not move the horizon at $r = h$, which remains at $\tilde{r} = \tilde{h}$.

Note, however, that while the original MK metric $g_{\mu\nu}$ has a linear potential γr , the corresponding Higgs-frame metric $\tilde{g}_{\mu\nu}$ has no term in \tilde{g}_{00} linear in \tilde{r} . Thus even though the Higgs field $S(r)$ declines only slightly from its central value S_0 , this has a significant effect on the shape of the potential and the resulting rotation curve. With B rising as $B \approx 1 + \gamma r$, S falls as $S/S_0 \approx 1 - \gamma r/2$, so that $S^2 B$ lacks a linear potential. While this result is demonstrated here for a point mass, rather than for a more realistic extended source structure, it indicates the potential danger when using the linear potential in the MK metric to fit galaxy rotation curves.

Fig. 2 further illustrates this point by showing the Higgs-frame potential $(S/S_0)^2 B$, and the corresponding rotation curve, for the same $10^{11} M_\odot$ point mass as in Fig. 1. The Higgs field is constant, by definition, in the Higgs frame. Because $a \approx 2/\gamma = 7.6 \times 10^{10}$ pc is by far the longest scale in the problem, r and $\tilde{r} = r a / (r + a)$ are nearly identical, and the Higgs-frame mass M and curvature K are essentially unchanged from their MK-frame counterparts β and κ . The Higgs-frame potential $(S/S_0)^2 B$ retains the Newtonian potential $-2\beta/\tilde{r}$ and the quadratic potential $-\kappa \tilde{r}^2$, but lacks a linear potential term. The rotation curve thus follows a Keplerian profile out to ~ 20 kpc, bending down as the quadratic potential takes hold, and the watershed radius, where $-\tilde{g}_{00} = (S/S_0)^2 B$ has a maximum, is now at $\tilde{r} = |\beta/\kappa|^{1/3} = 37.5$ kpc.

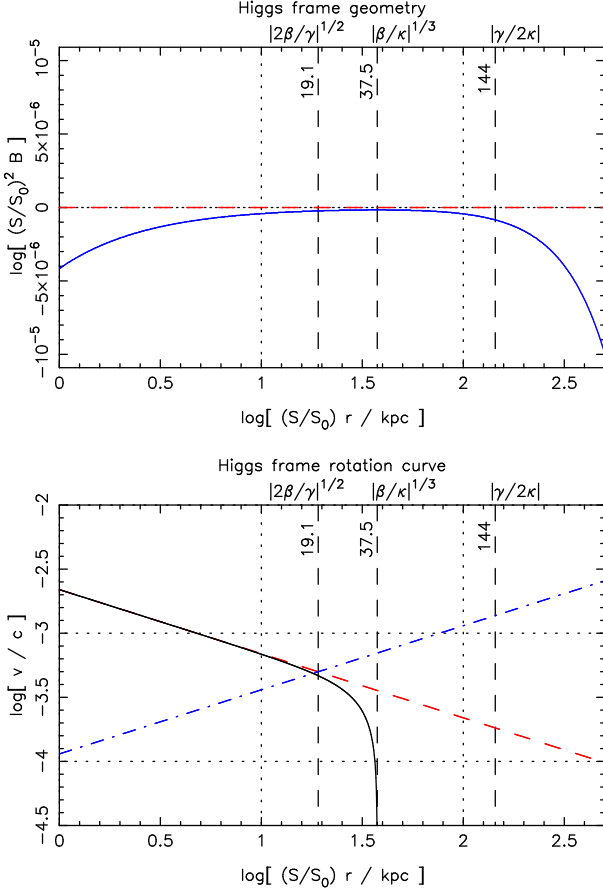


Figure 2. Same as in Fig. 1 but after a conformal transformation $\Omega(r) = S(r)/S_0$ stretches the geometry from the MK frame, where $B(r) = -g_{00} = 1/g_{rr}$, to the Higgs frame, where the Higgs field is constant. The Higgs-frame potential $\tilde{B} \equiv (S/S_0)^2 B$ has a maximum at the watershed radius $\tilde{r} \equiv (S/S_0) r = |\beta/\kappa|^{1/2} \approx 37.5$ kpc, outside which there are no stable circular orbits. Note that $B(r)$ has a rising linear potential γr , but this is effectively canceled by the decline in S^2 , so that the rotation curve is Keplerian out to ~ 20 kpc.

5 ASTROPHYSICAL TESTS

To really test CG with astrophysical observations is considerably harder than simply using geodesics of the MK metric with $B(r)$ sourced by matter. The source $f(r)$ in CG's 4th-order Poisson equation must include contributions from the Higgs halo $S(r)$, in addition to those from the matter (+radiation) energy density $\rho(r)$ and pressure $p(r)$. These are specified in the Higgs frame, $\tilde{\rho}(\tilde{r})$ and $\tilde{p}(\tilde{r})$, and moved to the MK frame using $\tilde{r} = r S(r)/S_0$, $\rho(r) = (S/S_0)^4 \tilde{\rho}(\tilde{r})$ and $p(r) = (S/S_0)^4 \tilde{p}(\tilde{r})$. For example, to model spherical structures similar to the matter distribution in galaxies and clusters, it may be appropriate to adopt a Hearnquist profile (Hearnquist 1990)

$$\tilde{\rho}(\tilde{r}) = \frac{\rho_0}{x(x+1)^3}, \quad (45)$$

with $x = \tilde{r}/r_0$ in units of the scale radius r_0 , and with $\rho_0 = M/(2\pi r_0^3)$ for total mass M . The enclosed mass profile is

$$M(\tilde{r}) = M \left(\frac{x}{x+1} \right)^2. \quad (46)$$

This Hearnquist profile $\tilde{\rho}(\tilde{r})$ is specified in the Higgs frame, then scaled by $(S/S_0)^4$ for use in the MK frame where the 4th-order Poisson equation and 2nd-order Higgs equation are more easily solved.

In the MK frame, $B(r)$ and $S(r)$ satisfy their equations of motion. The 4th-order Poisson equation for $B(r)$,

$$\frac{4\alpha}{r} (rB)'''' = S^3 \left(\left(\frac{1}{S} \right)'' + \frac{1}{B^2} \left(\frac{1}{S} \right)' \right) - \frac{3}{B} \left(\frac{S}{S_0} \right)^4 (\tilde{\rho} + \tilde{p}) \equiv 4\alpha f(r), \quad (47)$$

is convenient because solutions of the form

$$B(r) = w(r) - \frac{2\beta(r)}{r} + \gamma(r)r - \kappa(r)r^2 \quad (48)$$

can be found for extended sources $f(r)$ by integrating 1st-order equations, with appropriate boundary conditions:

$$\beta' = \frac{r^4}{12} f(r), \quad \beta(0) = \beta_0, \quad (49)$$

$$\gamma' = -\frac{r^2}{2} f(r), \quad \gamma(0) = \gamma_0, \quad (50)$$

$$\kappa' = -\frac{r}{6} f(r), \quad \kappa(\infty) = \kappa_\infty, \quad (51)$$

$$w' = \frac{r^3}{2} f(r), \quad w^2(r) = 1 - 6\beta(r)\gamma(r) + \frac{3r^4}{4\alpha} T_r^r(r). \quad (52)$$

The MK parameters, $\beta(r)$, $\gamma(r)$, $\kappa(r)$, $w(r)$, are then internal and/or external moments of $f(r)$. For non-singular structures, appropriate boundary conditions at the origin are $\beta(0) = 0$ and $\gamma(0) = 0$, though non-zero values may also be chosen for an unresolved central source such as a nucleon, a star, or a black hole. The curvature of the external 3-space is set by $\kappa(\infty)$. The 3rd-order constraint on w can be set any radius where T_r^r is known.

Note that even for an extended source $f(r)$, the first 3 derivatives of $B(r)$ evaluate as if the MK parameters were r -independent. For example:

$$B' = \frac{2\beta}{r^2} + \gamma - 2\kappa r - \frac{2\beta'}{r} + w' + \gamma' r - \kappa' r^2 \\ = \frac{2\beta}{r^2} + \gamma - 2\kappa r + \left(-\frac{1}{6} + \frac{1}{2} - \frac{1}{2} + \frac{1}{6} \right) r^3 f. \quad (53)$$

As a consequence, the Ricci scalar remains

$$\mathcal{R} = \frac{2(w(r)-1)}{r^2} + \frac{6\gamma(r)}{r} - 12\kappa(r), \quad (54)$$

and the 3rd-order constraint remains

$$W_r^r = \frac{w(r)^2 + 6\beta(r)\gamma(r) - 1}{3r^4} = \frac{1}{4\alpha} T_r^r. \quad (55)$$

Here T_r^r includes radial pressure from both matter (+radiation) and from the Higgs halo:

$$T_r^r = \frac{(\dot{S})^2 - 2S\ddot{S}}{6B} + \frac{B}{2} (S')^2 + \frac{SS'}{6} \left(B' + \frac{4B}{r} \right) \\ + \frac{S^2}{6} \left(\frac{B'}{r} + \frac{B-1}{r^2} \right) - \lambda S^4 + \tilde{p}_r \left(\frac{S}{S_0} \right)^4. \quad (56)$$

Because $f(r)$ depends on $B(r)$ and $S(r)$, the moment integrals for $B(r)$ must be iterated along with solving the 2nd-order Higgs equation for $S(r)$:

$$\frac{\ddot{S}}{B} = \frac{1}{r^2} (r^2 B S')' + \frac{\mathcal{R}}{6} S - \left(4\lambda + \frac{\tilde{\rho} - \tilde{p}_r - 2\tilde{p}_\perp}{S_0^4} \right) S^3, \quad (57)$$

with boundary conditions $S(0) = S_0$ and $S'(0) = S_1$.

Having solved for $B(r)$ and $S(r)$ in the MK frame, we move back to the Higgs frame, and use geodesics of the resulting Higgs-frame metric $\tilde{g}_{\mu\nu} = (S(r)/S_0)^2 g_{\mu\nu}$ to test CG in 3 ways:

1. galaxy rotation curves.
2. galaxy cluster potentials probed by X-ray gas.
3. lensing by galaxies and galaxy clusters.

For example, the circular orbit rotation curve is:

$$v^2 = \frac{d \ln(|\tilde{g}_{\theta\theta}|)}{d \ln(|\tilde{g}_{\theta\theta}|)} = \frac{d \ln(S B^{1/2})}{d \ln(S r)} = \frac{v_B^2 + v_S^2}{1 + v_S^2}, \quad (58)$$

where

$$v_B^2 = \frac{r B'}{2 B} = \frac{\frac{\beta}{r} + \frac{\gamma}{2} r - \kappa r^2}{w - \frac{2\beta}{r} + \gamma r - \kappa r^2} \quad (59)$$

is the rotation curve arising from the MK potential $B(r)$, as used by (Mannheim & O'Brien 2012), and $v_S^2 \equiv r S'/S$ implements the corrections arising from the Higgs halo profile $S(r)$.

One of the objections to CG is that for the MK metric with $\gamma > 0$ the linear potential causes light rays to bend away from the point mass, rather than toward it. But our results show that a rising MK-frame potential $B(r)$ is compensated by a corresponding decline in the Higgs halo $S(r)$. In light of this, the galaxy rotation curves may not in fact require $\gamma > 0$, and we may now reconsider adjusting the strength and sign of the linear potential when testing CG predictions for gravitational bending of light rays. It remains to be shown whether the effect of an extended source $f(r)$ appropriate to modelling galaxies and clusters can fit the light bending angles from lensing as well as the flat rotation curves. We hope to address this in future work.

6 CONCLUSIONS

The 4th-order field equations of Conformal Gravity have vacuum solutions that augment the Schwarzschild metric with linear and quadratic potentials (Mannheim & Kazanas 1989). This MK metric has been used to fit the rotation curves of a wide variety of galaxies with only 3 free parameters (Mannheim & O'Brien 2012).

We highlight two potential problems with using geodesics of the MK metric to study rotation curves of galaxies. First, the MK metric is a source-free solution to CG's 4th-order Poisson equation, but the conformally-coupled Higgs field makes an extended halo $S(r)$ that also contributes to the gravitational source unless it has a specific radial profile, $S(r) = S_0 a/(r+a)$. Second, since particle masses scale with the Higgs field, the Higgs halo $S(r)$ pushes test particles off geodesics of the MK metric.

To address these issues, we note that a conformal factor $\Omega(r) = S(r)/S_0$ stretches the metric to a form that makes the Higgs field constant. Test particles then follow geodesics of this stretched "Higgs-frame" metric.

For the analytic solution to the source-free CG equations (Brihaye & Verbin 2009), which is equivalent to the MK metric, we find that the effect of stretching the metric to the Higgs frame is to eliminate the linear potential that

is used to fit galaxy rotation curves. Thus the remarkable results of (Mannheim & O'Brien 2012), using geodesics of the MK metric to fit a large variety of galaxy rotation curves with just 3 parameters, may be testing an empirical model rather than the actual CG predictions.

We collect the equations and outline the procedure for astrophysical tests of CG in static spherical geometries. Specifically, the sources for CG's 4th-order Poisson equation include not only the energy density and pressure of distributed matter (stars+gas), and radiation if relevant, but also the associated Higgs halo $S(r)$. The resulting MK metric $g_{\mu\nu}$ must then be "stretched" to the Higgs frame metric $\tilde{g}_{\mu\nu} = (S/S_0)^2 g_{\mu\nu}$. The Higgs-frame geodesics then provide predictions for testing CG against observations.

Acknowledgements

KH would like to thank Amy Deacon, Aidan Farrell and Indar Ramnarine for hospitality at the University of the West Indies in Trinidad, Alistair Hodson, Alasdair Leggat, and Carl Roberts for helpful comments on the presentation, and the UK Science and Technology Facilities Council (STFC) for financial support through consolidated grant ST/M001296/1.

REFERENCES

- Brihaye, Y., Verbin, Y. 2009 Phys.Rev.D 80, 124048.
 Edery, A., Paranjape, M.B. 1998, Phys.Rev.D 58, 24011.
 Hearnquist, L., 1990, ApJ 356, 359.
 Mannheim, P.D. 1993, ApJ 419, 150.
 Mannheim, P.D. 1993, Gen.Rel.Grav. 25, 697.
 Mannheim, P.D. 1997, ApJ 479, 659.
 Mannheim, P.D. 2001, ApJ 561, 1.
 Mannheim, P.D. 2003, IJMPD 12, 893.
 Mannheim, P.D. 2006, Prog.Part.Nucl.Phys 56, 340.
 Mannheim, P.D. 2007, Phys.Rev.D 75, 124006.
 Mannheim, P.D. 2011, Gen.Rel.Grav. 43, 703.
 Mannheim, P.D. 2012, Phys.Rev.D 85, 124008.
 Mannheim, P.D., Kazanas, D. 1989, ApJ 342, 635.
 Mannheim, P.D., Kazanas, D. 1991, Phys.Rev.D, 44, 417.
 Mannheim, P.D., O'Brien, J.G. 2012, Phys Rev D 85, 124020.
 Nesbet, R.K. 2011, MPLA 26, 893.
 Pireaux, S. 2004, Class.Quant.Grav 21, 1897.
 Rubin, V.C., Ford, W.K., Thonnard, N. 1978, ApJL 225, L107.
 Sultana, J., Kazanas, D. 2010 Phys.Rev.D, 81, 7502.
 Tully, R.B., Fisher, J.R. 1977, A&A 54, 661.
 Villanueva, J.R. & Olivares, M. 2013, JCAP 06, 40.
 Wehus, I.K., Ravndal, F. 2007, J.Phys.Conf.Ser 66, 012044.
 Wood, J., Moreau, W. 2001, arXiv:gr-qc/0102056

This paper has been produced using the Royal Astronomical Society/Blackwell Science L^AT_EX style file.